PHILOSOPHICAL TRANSACTIONS OF THE ROYAL SOCIETY B BIOLOGICAL SCIENCES

Quantification in tissue near–infrared spectroscopy

D. T. Delpy and M. Cope

Phil. Trans. R. Soc. Lond. B 1997 **352**, 649-659
doi: 10.1098/rstb.1997.0046

Quantification in tissue near-infrared spectroscopy

D. T. DELPY AND M. COPE

Department of Medical Physics and Bioengineering, University College London, Shropshire House, 11–20 Capper Street, London WC1E 6JA, UK

SUMMARY

In near-infrared spectroscopy (NIRS) of tissue, light attenuation is due to: (i) absorption from chromophores of fixed concentration, (ii) absorption from chromophores of variable concentration, and (iii) light scatter. NIRS is usually concerned with trying to quantify the concentrations of chromophores in category (ii), in particular oxy- and deoxyhaemoglobin (HbO_2 and Hb) and cytochrome oxidase.

In the absence of scatter the total light absorption in the medium is a linear sum of that due to each chromophore. In a scattering medium like tissue, this linear summation is distorted because the optical path length at each wavelength may differ. This distorted spectrum is then superimposed upon a further wavelength-dependent attenuation arising from light loss due to scatter, which is a complex function of the tissue absorption and scattering coefficients (μ_a and μ_s), scattering phase function, and tissue and measurement geometry. Consequently, quantification of NIRS data is difficult.

Over the past 20 years many differing approaches to quantification have been tried. The development of methods for measuring optical path length in tissue initially enabled changes in concentration to be quantified, and subsequently methods for absolute quantification of HbO_2 and Hb were developed by correlating NIRS changes with an independent measurement of arterial haemoglobin saturation. Absolute determination of tissue optical properties, however, requires additional information over and above the detected intensity at the tissue surface, which must then be combined with a model of light transport to derive μ_a and μ_s. The additional data can take many forms, e.g. the change in intensity with distance, the temporal dispersion of light from an ultrashort input light pulse, or phase, and modulation depth changes of intensity-modulated light. All these approaches are now being actively pursued with considerable success. However, all the approaches are limited by the accuracy of the light transport models, especially in inhomogeneous media.

1. INTRODUCTION

In vivo near-infrared spectroscopy (NIRS) utilizes light in the wavelength range 700–1000 nm to transilluminate large sections of tissue. This choice of wavelength follows from the absorption spectra of the major tissue chromophores. Water, the dominant tissue chromophore, absorbs strongly below 300 nm and above 1000 nm. In the visible part of the spectrum between 400 and 650 nm, absorption from haemoglobin and melanin dominates, leaving only the NIR region where overall absorption is sufficiently low for light to be detected across many centimetres of tissue. In the NIR many chromophores still absorb light, but there are only three of clinical importance that exhibit oxygenation-dependent absorption, these being oxyhaemoglobin (HbO_2) and deoxyhaemoglobin (Hb) in the red blood cells and the oxidized form of cytochrome oxidase (CytOx), an enzyme involved in oxidative metabolism and found in the cell mitochondrial membrane. Figure 1 shows the NIR absorption spectra of these compounds. (For reasons discussed later, the cytochrome spectrum shown here is the difference spectrum between the oxidized and reduced form of the enzyme.) The aim of NIR spectroscopy is to quantify the concentrations of these chromophores in tissue. It is worth noting that with the exception of the relatively sharp spectral feature of Hb at 760 nm, the spectra are relatively broad and featureless. In addition, the cytochrome oxidase absorption is a factor of ten less than that arising from the haemoglobin at *in vivo* concentrations.

It was in 1977 that Jöbsis first described the *in vivo* application of NIRS to monitor changes in the oxygenation of the brain in the intact cat head. In this paper Jöbsis (1977) showed that changes in the spectrum measured across the head could be related to changes in chromophore concentration using the known spectra of haemoglobin and cytochrome oxidase (Wray *et al.* 1988) and applying the Beer–Lambert Law. However, quantification of the changes was not possible because the path length of the light in the tissues was unknown, although in animals the 'total labile signal' could be estimated through manipulation of the inspired oxygen concentration. The paper highlighted the major problem of NIRS data quantification which arises from the fact that light attenuation in tissue comes not just from absorption changes, but also from light scattering; this not only introduces an unknown light loss, but also results in a non-linear relationship between absorption changes and the resulting attenuation changes. In the NIR, the

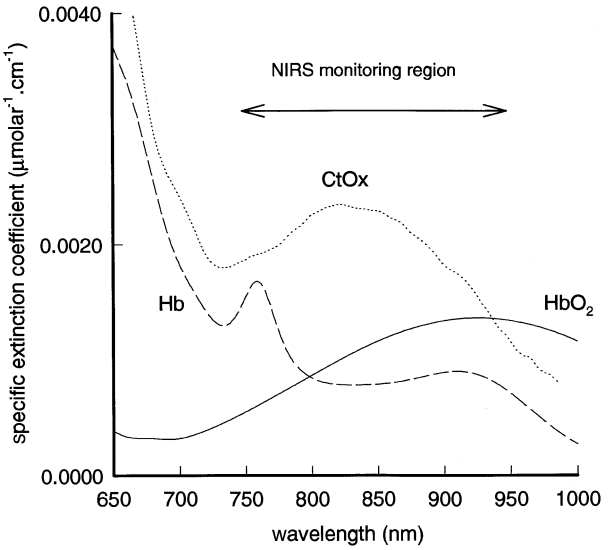

Figure 1. Specific extinction coefficient for Hb, HbO_2 and CytOx (oxidized minus reduced) in the NIR. Note that *in vivo*, the contribution of the cytochrome to overall absorption is considerably less than that of the haemoglobin because of its lower concentration.

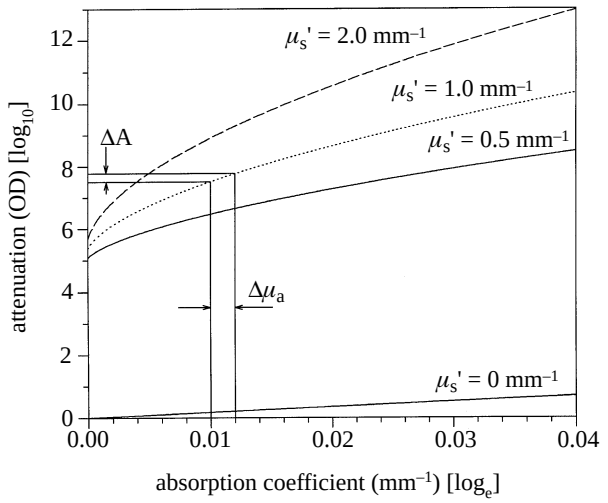

Figure 2. Predicted relationship between measured attenuation and absorption coefficient across 4 cm of tissue with three different values of μ_s' and for the non-scattering case. Note the difference in the log base normally used to define the parameters.

transport scattering coefficient (μ_s') of most tissues is much larger than the absorption coefficient (μ_a). The typical value for μ_s' is around 1 mm^{-1} (range 0.5–10 mm^{-1}) whereas μ_a lies in the range 0.005–0.02 mm^{-1} (Cheong *et al.* 1990). The consequence of the high μ_s' is that the light entering the tissues rapidly becomes a diffuse photon density which then propagates through the tissue. The resulting light distribution can be described by the diffusion equation (Patterson *et al.* 1989; Arridge *et al.* 1992), from which it is possible to calculate the expected relationship between total attenuation A ($\log(I_0/I)$) and change in tissue absorption; figure 2 illustrates simulated results for a tissue slab 4 cm thick. Four important features can be seen in this figure. First, the attenuation is not zero when the absorption is zero. This residual attenuation arises from the light loss due to scattering, its exact value depending on the tissue and measurement geometry as well as μ_s'. Second, the attenuation versus absorption relationship depends on the exact value of μ_s'. Third, the relationship is non-linear, and depends on both μ_s and μ_a. Finally, the optical path length in the tissue (equivalent to the slope of the attenuation versus absorption curves) is greater than the optode spacing, and varies with μ_s' and μ_a.

Over the past 20 years, developments in the NIRS field have concentrated on solving the problems of data quantification, as this allows NIRS measurements to be compared between different patient groups, species and other measurement modalities, such as positron emission tomography. The published NIRS literature has recently been reviewed (Wahr *et al.* 1996), and technical developments in the field are comprehensively covered in the SPIE proceedings (*Proc. SPIE* 1991, 1993, 1995).

2. NIRS MEASUREMENT INSTRUMENTATION

Many different types of measurement instrumentation have been developed, and in this review we will consider them as falling into only three general categories: continuous intensity, time resolved and intensity modulated. These are illustrated schematically in figure 3.

(*a*) *Continuous intensity instruments*

These instruments, which include the earliest NIR spectrometers, generally employ either a filtered white light source or multiple discrete wavelength sources (laser diodes or light emitting diodes, LEDs), and only measure the transmitted intensity using either a photomultiplier (PMT), photodiode or avalanche photodiode (APD) detector (Giannini *et al.* 1982; Wickramsinghe *et al.* 1986; Cope *et al.* 1988). Most frequently the source and detector are linked to the tissue using fibre optics, although in some photodiode-based systems, the detector is placed directly on the skin. Major technical developments in these instruments have involved increasing the light input to the tissues (commensurate with the allowable regulatory limits), maximizing of instrumental sensitivity to enable small changes in attenuation to be accurately measured and system optimization to ensure extremely low long-term drift. More recently, highly multi-wavelength systems utilizing cooled CCD array detectors and white light sources have been used (Cope *et al.* 1989).

(*b*) *Time-resolved instruments*

In these instruments, light is input to the tissues in the form of an ultrashort (picosecond) pulse, and the emerging intensity (the temporal point spread function, TPSF) detected as a function of time, again with picosecond resolution (Chance *et al.* 1988*a*; Delpy *et al.*

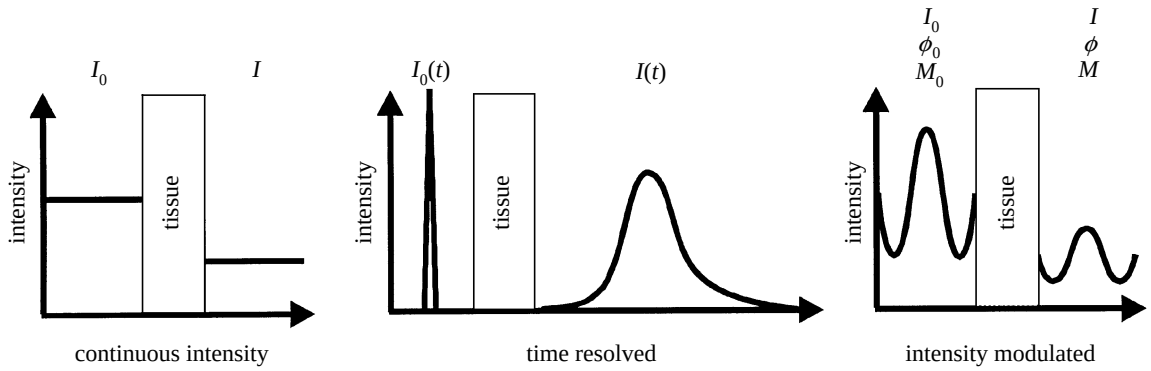

Figure 3. Schematic illustration of the three main types of NIRS instrumentation.

1988). The ultrashort pulse requirements of the source restrict these in general to semiconductor, dye or solid state lasers, which produce only discrete wavelengths. Pulsed broadband light sources are available, but at present these are large laboratory-based devices and hence difficult to apply in a clinical environment. Multiwavelength measurements therefore require either multiple sources, or tunable sources and sequential measurements, and in the latter case, a rapid wavelength change is important because the physiological state of the tissue should not alter during the measurement time. Two detection schemes have been applied to this type of measurement. The first uses the synchroscan streak camera, which, in principle, allows intensity to be detected at several different points on the tissue through the use of separate optical fibres mounted across its entry slit (the disadvantage being that the amount of light detected falls in proportion to the detecting fibre area). The streak camera has the advantages of speed and flexibility, but it is large and expensive and has a limited dynamic range (approximately 1000). The alternative detection scheme is time-correlated single photon counting (TCSPC) in which a photon counting detector (PMT, microchannel plate PMT or APD) detects and sorts the received photons by their time of arrival. The distribution of arrival times of a large number of photons is the TPSF. This technique has the advantage of requiring smaller and cheaper components and, providing the maximum photon count rate is not exceeded, is linear over a wide dynamic range. Its disadvantages are its slow speed, the rate of photon detection being determined by the instrumental count rate, and that multiple detection requires either additional detectors or a multiplexing scheme with a consequent reduction in data collection rate per channel.

The TPSF is essentially the 'impulse response' of the tissue, and in principle the optical properties of the tissues can be determined from it analogous to electronic engineers determining the 'equivalent circuit' of a black box from its response to a voltage or current impulse. It is important to note that the properties obtained in this way (μ_a, μ_s', refractive index, etc.) depend upon having an accurate model for light transport in the tissues, and only represent the averaged values for those parameters that best match the measured data.

(*c*) *Intensity-modulated instruments*

In these instruments, the light source (usually a laser diode or LED) is intensity-modulated at radio frequencies (RF), and measurement is made not only of the detected light intensity, but also its phase shift (Φ) and modulation depth (M) with respect to the input light (Lackowicz *et al*. 1988; Chance *et al*. 1990; Duncan *et al*. 1993; Fantini *et al*. 1995). It is also possible to build instruments based on modulated white light sources and gain modulated area detectors (Patterson *et al*. 1994), but the light losses associated with these technologies limit their use to measurement through relatively thin tissue sections. The detection of small changes in Φ or M at RF is difficult, so almost all these instruments employ some down-conversion scheme to bring the RF signal down to an intermediate frequency (IF) or audio frequency (AF) where conventional phase detection techniques can be applied. In general, two different schemes have been employed for this demodulation. In the first (using PMT detectors), the detector gain is modulated at a reference frequency offset by a few kHz from the light source modulation frequency resulting in direct demodulation in the detector. The detector output is then an AF signal at the difference frequency (Chance *et al*. 1990). This scheme can, in principle, be applied over a broad RF range, but requires many watts of RF power to provide the 30–100 V modulation typically required at the PMT dynode. This technique can, however, be very efficient at a single frequency where the dynode is made part of a resonant circuit at the applied RF. The second scheme does not gain modulate the detector, but the detected signal is subsequently fed into a double balanced mixer together with the reference RF signal and hence down-converted to AF (Duncan *et al*. 1993). This scheme is simpler to apply over a broad range of RF as it is easier to obtain impedance matching over a broad frequency range and it requires lower RF powers (around 10 mW).

It has been demonstrated (Patterson *et al*. 1989; Arridge *et al*. 1992) that for typical tissues, and frequencies below 200 MHz, Φ is linearly related to the average optical path length. Knowledge of phase then enables direct conversion of changes in attenuation into changes in chromophore concentration. Above 200 MHz (the dispersion regime), a linear relationship between path length and phase shift no longer applies.

3. MEASUREMENT TYPES

Associated with each type of instrumentation is an equally wide range of types of measurement that can be made with them. Table 1 is an illustrative matrix of some of the many possible combinations. It is not meant to be comprehensive, but represents many of the more commonly made measurements. These are briefly reviewed below.

(*a*) *Continuous intensity instruments*

(i) *Intensity change at fixed spacing*

This is the type of measurement made in the earliest clinical NIRS studies (Brazy *et al*. 1985; Ferrari *et al*. 1986). As the detected light intensity contains an unknown light loss due to the tissue scattering and measurement geometry (figure 2), these early measurements disregarded the absolute level of the detected light, and instead measured only the changes in attenuation (ΔA) from some arbitrary start time. The assumption was then made that small changes in $\mu_a$were approximately linearly related to the measured ΔA enabling the Beer–Lambert law to be applied, the optical path length being an unknown but constant value. If it is further assumed that changes in attenuation can only arise from variations in the concentration of Hb, HbO_2 and the redox state of CytOx, then these can be separately identified from measurements of ΔA made at three different wavelengths. Three wavelengths are needed if it is assumed that the total CytOx concentration is constant and only its redox state alters (in which case only the difference absorption spectrum between the oxidized and reduced forms of CytOx is required). Quantification of the magnitude of the changes requires that we know the factor by which the optical path length is increased due to scattering (known as the differential path length factor (DPF), because it relates differences in attenuation to differences in concentration). This factor can be determined from time-resolved techniques to determine the mean 'time of flight' of an ultrashort pulse of light through the tissues (Delpy *et al*. 1998). From figure 2 we know that the path length also depends upon μ_a and μ_s', both of which will, in general, be wavelength-dependent. Experimental measurements of DPF and its wavelength dependence made on a range of tissues have shown that for a given tissue the DPF is approximately constant as a function of optode spacing (Van der Zee *et al*. 1992; Essenpreis *et al*. 1993). This data enabled researchers to obtain for the first time quantitative changes in concentrations from the measured ΔA and knowledge of the optode spacing (Wyatt *et al*. 1986). From these data it has proven possible to derive quantitative values for some other physiological variables. For instance, haemoglobin saturation can be derived from the ratio $\Delta HbO_2/\Delta(HbO_2 + Hb)$ during physiologically induced changes in total blood volume. These alterations in blood volume can be either spontaneous respiratory-related changes (Elwell *et al*. 1996), ones induced by variations in venous pressure (Wyatt *et al*. 1986; Skov *et al*. 1993) or venous drainage from the organ of interest (Yoxall *et al*. 1995), or in the case of the fetus, variations in intrauterine pressure during labour (Peebles *et al*. 1992; Aldrich *et al*. 1994). Tissue oxygen consumption can also be quantified from the rate of decline of HbO_2 during transient ischaemia induced either by an inflatable cuff or isometric exercise (Cheatle *et al*. 1991; De Blasi *et al*. 1994, 1995).

Methods of absolute quantification of the Hb and HbO_2 signals (i.e. determining the baseline from which the quantified changes are occurring) have also now been developed by making known small perturbations in the blood oxygen saturation (measured by pulse oximetry), and correlating the NIRS measured changes to these. This has enabled the absolute measurement of tissue blood flow and blood volume (Edwards *et al*. 1988; Wyatt *et al*. 1990). Although extremely useful, all these techniques require some physiological change to be made, often by deliberate intervention. This is often not possible in many clinical circumstances, and alternative techniques providing quantification without any intervention have been sought. Note also that none of the methods described enables absolute quantification of CytOx concentration or redox state.

(ii) *Differential spectra at fixed spacing*

Developments in cooled CCD array detectors over the past decade have made possible the design of highly sensitive fibre-coupled spectrometers capable of measuring complete spectra in the 500–1000 nm range across many centimetres of tissue (Cope *et al*. 1989). These instruments have been invaluable in obtaining accurate *in vivo* spectra enabling the development and testing of the algorithms used to convert the measured changes in attenuation to changes in chromophore concentration (Wray *et al*. 1988; Cope *et al*. 1991;

Table 1. *An illustrative matrix of some possible combinations of NIRS instrumentation and measurement type*

type of instrument	measurement		
continuous intensity	fixed spacing $\Delta I(\lambda)$ plus DPF data	fixed spacing $(dI/d\lambda)$; $(d^2I/d\lambda^2)$	multiple spacing $\Delta I(\lambda)$ vs distance
time resolved	fixed spacing complete $I(t)$ data (i.e. TPSF)	fixed spacing log $I(t)$ final slope	fixed spacing $I(t) \Rightarrow I(t_0)$ extrapolation
intensity modulated	fixed spacing I; Φ; M; vs frequency	fixed spacing ΔI; $\Delta\Phi$; ΔM; vs $\Delta\ \mu_a$	multiple spacing ΔI; $\Delta\Phi$; ΔM; vs distance

Matcher *et al.* 1995*a*). However, the increased spectral information provides many other advantages. The first is the ability to accurately measure the absorption peaks due to water in the tissues. In the NIR, the water spectrum contains three major features, a prominent peak centred around 965 nm and two other small 'steps' in absorption around 820 and 740 nm. The 965 peak is large enough to allow accurate curve-fitting of its shape to the known spectrum of 1 cm of pure water. As the concentration of water in the tissues is often known to an accuracy of a few per cent, it is possible from the ratio of the peak amplitudes and the known optode spacing to estimate the optical path length at 965 nm (Cope *et al.* 1989).

Subsequently, an improved method for path length estimation using the second derivative of the measured spectrum was developed. The principle of this technique is that if the measured spectrum sits on an unknown constant attenuation, then this can be removed by taking the first derivative of the spectrum with respect to wavelength. If there is an additional unknown, but linearly wavelength-dependent, attenuation present, this will appear as a constant in the first derivative, which can be removed by taking the second derivative. This should leave a flat spectrum containing only features corresponding to the second derivative of the absorption spectra of any chromophores in the tissue. In the NIR, the second derivative of the water spectrum has three components corresponding to the previously mentioned features. Hb has a large feature corresponding to the 760 nm absorption peak, but HbO_2 and CytOx have negligible features. In an early study using this technique (Ferrari *et al.* 1989), the Hb feature from spectra measured with optodes placed across the sagittal sinus on the intact dog head was shown to correlate closely with sagittal sinus haemoglobin saturation. In a subsequent study, the water features were used to estimate the optical path length at three wavelengths and a good correspondence shown between these and path lengths obtained by 'time of flight' measurements (Matcher *et al.* 1994). However, in addition, if the tissue water content is known, then the absolute Hb concentration can be obtained from the ratio of the Hb to water spectral components (Cooper *et al.* 1996).

(iii) *Intensity change at multiple spacing*

If the intensity of the light emerging from the tissues is measured as a function of optode spacing, then it is in principle possible to fit these data to a model of light transport and hence derive the μ_a and μ_s' of the tissues. The results from this technique depend critically on the accuracy of the model and its applicability to the tissue and measurement geometry. One early application of this technique was the estimation of the optical properties of dental enamel by fitting the experimental data to a diffusion model for an infinite slab (Groenhuis 1983*a*, *b*). Farrell *et al.* (1992) used the method to measure reflectance spectra as a function of distance on tissues, μ_a and μ_s' being derived from these data by comparison with a table of reflectance as a function of μ_a and μ_s' generated using either a Monte-Carlo or diffusion equation model. Measurement of intensity as a function of distance has also been adapted to the more 'conventional' type of NIR spectrometer employing four photodiode detectors, each a small distance from each other (Matcher *et al.* 1995*b*). If the wavelength dependence of μ_s' in the tissues is known, then the wavelength dependence of μ_a can be calculated from the change in intensity as a function of spacing, from which the absolute ratio of HbO_2 to Hb and hence average tissue saturation can be derived. Experimental measurements of μ_s' versus wavelength for various tissues showed that although the absolute values of μ_s varied considerably, the wavelength dependence was remarkably similar for all tissues (Matcher *et al.* 1997). Figure 4 shows data for mean forearm saturation measured by this technique during cuff occlusion. A point to note is the low value obtained for the resting saturation, which from physiological data one might expect to be in the 75–80 % range. Differences from the expected values have been observed in measurements of tissue saturation made using the majority of the absolute quantification techniques described in this paper, although they all produce excellent agreement in laboratory studies on infinite homogeneous phantoms. The reasons for this discrepancy are discussed in §4.

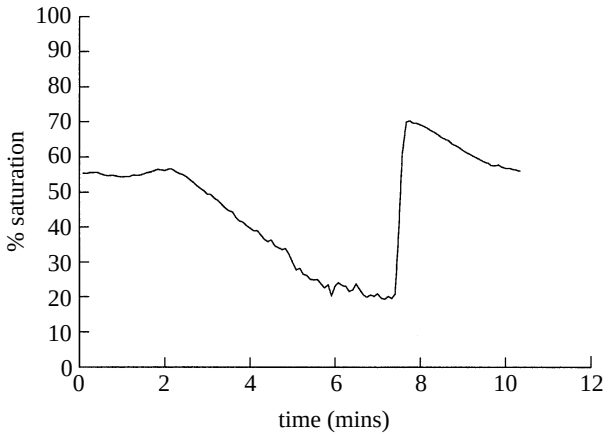

Figure 4. Mean forearm haemoglobin saturation measured by an NIR spectrometer employing four photodiode detectors, each a small distance apart, during arterial cuff occlusion and release (Matcher *et al.* 1995*b*).

(*b*) *Time-resolved instruments*

(i) *TPSF measurement at fixed spacing*

Using either a streak camera or TCSPC techniques, the complete TPSF of the tissue can be measured, and by fitting this to an appropriate model of light transport the values for μ_a and μ_s' can be estimated. Although normally requiring bulky equipment, a compact portable instrument using pulsed semiconductor laser diode sources and miniaturized TCSPC hardware has recently been described (Miwa *et al.* 1995). With this, the authors have shown that they can correctly measure the μ_a and μ_s' of an infinite homogeneous phantom. In experimental measurements on the arm, the derived tissue saturation is again slightly lower than expected, at 65–70 %. In an experimental study, Madsen *et al.* (1992) looked at the errors introduced by applying the diffusion equation solution for an infinite slab to other

PHILOSOPHICAL TRANSACTIONS OF THE ROYAL SOCIETY B BIOLOGICAL SCIENCES

geometries (cylinders and spheres), showing that errors increase as the object size decreases (due to light loss at the boundaries).

(ii) *Log(TPSF) slope at fixed spacing*

A typical tissue TPSF is characterized by a relatively rapidly rising intensity, peaking around 600–1000 ps and then a slow decay often several nanoseconds in duration (Chance *et al.* 1988*a*). When plotted on a logarithmic scale, the slowly decaying final slope is observed to be almost linear and, from diffusion theory, a simple relationship between the asymptotic limit of this final slope and the tissue μ_a can be obtained (Chance *et al.* 1988*b*; Sevick *et al.* 1991). Determination of this slope is much easier than measurement of the complete TPSF, and does not require as high a temporal resolution from the measurement system. This late emerging light has also probed deeper into the tissues, which can be advantageous, especially in cerebral studies, but unfortunately it is also the most likely to have reached the tissue boundary. This loss at the boundary leads to an increased rate of decay and hence to an error in the estimate of tissue μ_a similar to that described in the section above. Theoretical studies have also shown that in a non-homogeneous medium, the latest arriving photons tend to have come from the tissue with the lowest μ_a, leading to a further error in the average μ_a (Haselgrove *et al.* 1992).

(iii) *Temporal extrapolation at fixed spacing*

Two further methods of analysing the TPSF data have been proposed. The first has been called the 'microscopic Beer–Lambert law' (Hasegawa *et al.* 1991). In this, the TPSF of the tissue is measured at two different wavelengths and then the ratio of the intensities at corresponding times calculated. As time can be related to distance (knowing the speed of light and tissue refractive index), the resulting plot is essentially attenuation ratio as a function of distance (i.e. OD mm^{-1}, the units of absorption coefficient). Changes in chromophore concentration can be calculated from these if the difference in the tissue chromophore specific absorption coefficients is known and assuming that the scattering coefficient is constant over the wavelength measurement range. As with many of the other techniques described in this article, the method works well on homogeneous scattering phantoms, showing a Beer–Lambert-type relationship over a large range of measurement times (Oda *et al.* 1996).

A variant of this technique takes the above attenuation ratio versus time data and then extrapolates the resulting linear relation back to a time when the first (potentially unscattered) light would have emerged from the tissues (Yamada *et al.* 1993*b*). The attenuation at this point is theoretically the absorption ratio one would obtain in the absence of scattering. This is the so called temporally extrapolated absorbance method (TEAM). Although the absolute absorption coefficients obtained in this manner are slightly in error of the true values, the TEAM technique has proved useful in work on NIR imaging of tissues (Yamada *et al.* 1993*a*).

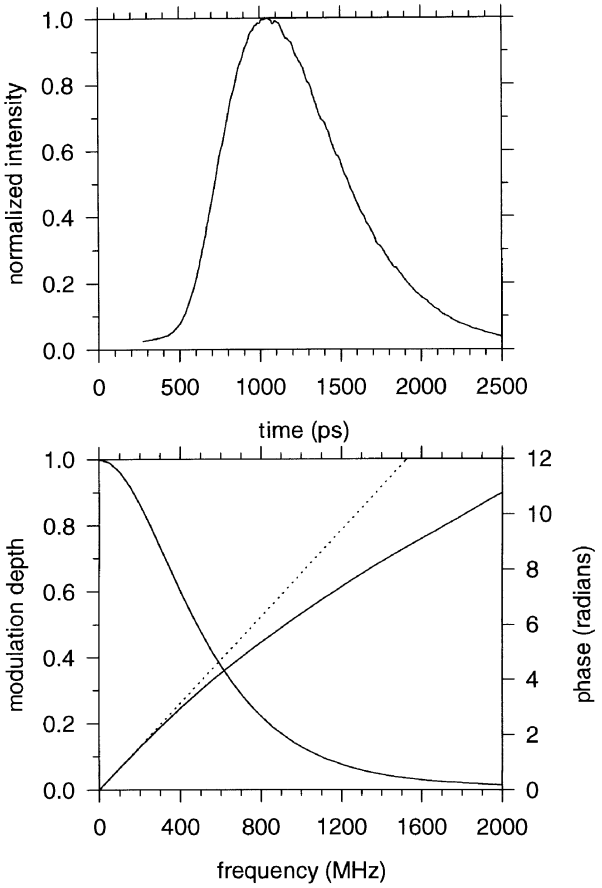

Figure 5. A TPSF measured across 4 cm of the adult head together with the corresponding Φ and M data obtained from its Fourier transform (the dotted line represents the linear Φ versus frequency relationship calculated from the mean time).

(*c*) *Intensity-modulated instruments*

(i) *Intensity, phase and modulation at fixed spacing versus frequency*

The information contained in the TPSF through time-resolved measurements can also be obtained in the frequency domain, the relation between the time and frequency information being the well known Fourier transform (Sevick *et al.* 1991; Duncan *et al.* 1993). Figure 5 shows a TPSF measured across 4 cm of the adult head together with the corresponding Φ and M data obtained from its Fourier transform. It can be seen that M has fallen to around 1% of its original value at approximately 2 GHz. In principle, therefore, one could obtain the same information as is found in the TPSF from a measurement of A, Φ and M from DC to 2 GHz. Unfortunately, the majority of PMTs have a practical working frequency limit (−3 dB) of approximately 500–700 MHz, beyond which the considerably more expensive microchannel plate PMT must be used, which is limited to approximately 3 GHz (Lakowicz *et al.* 1986). APD-based systems that can work up to 1 GHz have been designed, but their advantage of low cost and ruggedness is offset by their small detection area, which limits them to measurements across thinner sections of tissue (Madsen *et al.* 1994). Two studies have looked at the possibility of fitting Φ and M data measured over a limited

PHILOSOPHICAL TRANSACTIONS OF THE ROYAL SOCIETY B BIOLOGICAL SCIENCES

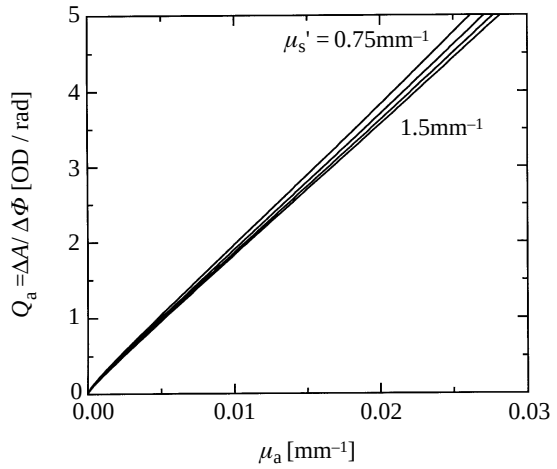

Figure 6. The predicted change in the ratio Q_a ($= (\partial A/\partial \mu_a)/(\partial \Phi/\partial \mu_a)$) for measurements across 3 cm of tissue as a function of μ_a for a range of different μ_s' values (Kohl *et al*. 1996).

frequency range (1 MHz–1 GHz) to a diffusion model and hence obtaining estimates of μ_a and μ_s'. (Duncan *et al*. 1993; Madsen *et al*. 1994).

(ii) *Intensity phase and modulation change at single frequency and fixed spacing*

Absolute measurement of A, Φ or M is technically more demanding than measuring changes in these quantities, so much work has gone into developing methods for deriving μ_a and μ_s' from changes in these parameters. One extremely promising recent development is a technique that uses ratios of the change in A, Φ and M with variation in tissue μ_a (Kohl *et al*. 1996). From diffusion theory, expressions for $\partial A/\partial \mu_a$, $\partial \Phi/\partial \mu_a$, and $\partial M/\partial \mu_a$ can be derived and hence the ratios of these parameters examined as a function of absolute μ_a and μ_s'. These show that some ratios are very insensitive to variations in μ_s. Figure 6 illustrates one such relationship. The implication of this observation is that if one can induce a small change in tissue absorption, then from a measurement of the ratio one can estimate the tissue μ_a without needing to accurately know μ_s'. In the case of the ratio Q_a ($= (\partial A/\partial \mu_a)/\partial \Phi/\partial \mu_a)$), experimental measurements have shown that variations in the assumed μ_s' of $\pm 50\,\%$ result in errors in the estimate of μ_a of only $\pm 4\,\%$. As mentioned in §3(*a*)(i), it is quite simple to induce small changes in blood volume or oxygenation (and hence μ_a), and indeed spontaneous small changes are frequently seen in clinical monitoring.

(iii) *Intensity phase and modulation change at single frequency and multiple spacing*

In §3*a*(iii) a quantification method using continuous intensity as a function of spacing was described. A similar technique can also be applied to intensity modulated measurements, the measured parameters being the change in A, Φ or M with distance. A relatively simple instrument for performing these measurements has been described using a single fibre coupled PMT detector and intensity modulated LED light sources (Fantini *et al*. 1995). The measured data is again fitted to an equation derived from diffusion theory, enabling in principle, both μ_a and μ_s' to be determined. As with the other systems described previously, the instrument works well on infinite homogeneous media, but when used to measure mean tissue saturation, again produces changes which underread true values.

4. FURTHER QUANTIFICATION PROBLEMS

(*a*) *Differences in tissue volumes probed by different instruments*

Using diffusion theory or alternative methods, such as Monte -Carlo modelling (Wilson *et al*. 1983; Hiraoka *et al*. 1993), we can now estimate for various tissue and measuring geometries, the volume of tissue interrogated by the detected light. These regions have been termed photon measurement density functions (PMDFs). If, for a given tissue and measuring geometry, we examine the PMDF for various different types of measurement (intensity, mean time, Φ, M, etc.), we see that these are, in fact, different. This is demonstrated in figure 7, which shows the continuous intensity and mean time PMDFs estimated for light travelling through the adult head, the source–detector spacing being 4.5 cm. The data were calculated using a finite element implementation of the time-dependent diffusion equation (Arridge *et al*. 1993), the tissue geometry being derived from a CT image of the head. In this simple illustrative example the head was only partitioned into two tissue types, an outer layer consisting of skin and skull, and an inner layer of brain. It can be clearly seen that in the case of the intensity measurement, the tissues contributing to the signal are much closer to the surface of the head than those contributing to the measurement of mean time (or phase). This difference in interrogated volumes does not only apply to the head, but is observed in other tissue types and in homogeneous tissues (Sevick *et al*. 1994). A consequence of this observation is that if *in vivo* measurements are made on the same tissues with instruments measuring different types of data, one would not be surprised to obtain differences in calculated μ_a, μ_s' or mean tissue saturation because the data will actually be coming from different tissue volumes which could be in differing physiological states. This has significant consequences in the planning of comparative trials between differing types of instrument.

(*b*) *Tissue geometry*

Figure 7 also illustrates the other consequence of the differing PMDFs, namely that as a result of tissue inhomogeneity, signals may actually be obtained from totally different tissue types. This is obviously not a problem when the optodes can be placed on a homogeneous tissue, but there is no such tissue (other than skin, which is itself a layered structure) that can be interrogated non-invasively without the light having

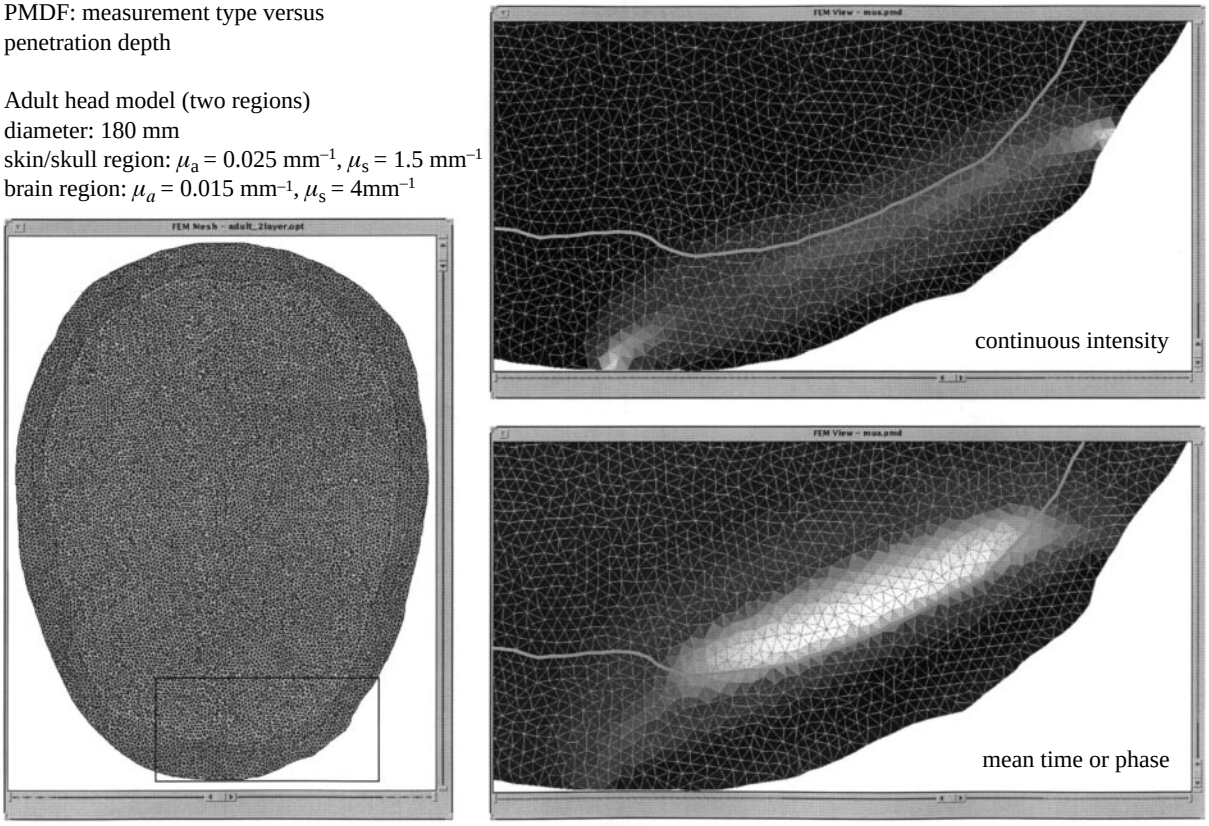

Figure 7. Continuous intensity and mean time PMDFs estimated for light travelling through the adult head. The data was calculated using a finite element implementation of the time-dependent diffusion equation, the source–detector spacing being 4.5 cm.

to pass through some intervening layer before entering the tissue of interest. Some authors have attempted to overcome this problem by combining measurements made at several different optode spacings in a way that it is hoped will cancel out the effects of the overlying tissue (McCormick *et al*. 1991; Germon *et al*. 1997). This technique has been applied in particular to measurements made on the adult head where the overlying skin and bone represent a significant tissue thickness (*ca*. 1 cm) compared to the optode spacing (typically 4–6 cm), although the results obtained have been very variable (Germon *et al*. 1994; Pollard *et al*. 1996).

(*c*) *Applicability of the diffusion equation*

Almost all the techniques described in this paper use equations based upon diffusion theory to derive values for μ_a and μ_s' from the data measured by the differing types of instrument. Diffusion theory is only applicable in cases where $\mu_s' \gg \mu_a$ and the optode spacing is $\gg 1/\mu_s'$, which is almost always true for all tissues in the NIR. There are, however, two major areas of concern. The first of these is the case of measurements made on the head, where a clear, non-scattering layer of cerebrospinal fluid lies between the inner skull table and the brain surface. Diffusion theory cannot be applied in this region, which means that alternative methods such as Monte-Carlo modelling must be employed, which are slow and computationally intensive (Okada *et al*. 1995, 1997). Recently, however, a hybrid diffusion/radiosity model has been described, which enables clear layers to be included in finite element models (Firbank *et al*. 1996). Results from this, corroborated by Monte-Carlo modelling show that the clear CSF layer has a considerable effect on the light distribution, leading to a reduction in the depth of light penetration into the brain, especially in the adult head. The second problem relates to a further assumption that is made in diffusion theory, namely that the tissues are homogeneous and scatter isotropically on a microscopic scale. Although this is obviously not true for tissue, diffusion theory has been remarkably successful in describing the experimentally observed light distributions, especially across many centimetres of tissue. However, in a recent careful study, measurements were made of the point spread function of light across slabs of various tissues *in vitro*, and the results compared to precise Monte-Carlo model predictions. The study showed that a good match between experiment and predictions could be obtained for liver and muscle tissue, but not for adipose tissue and brain (Bevilacqua *et al*. 1995; Marquet *et al*. 1995). The reasons for this discrepancy have not yet been determined, but may be due to anisotropy of scatter arising from the structural properties of these tissues.

5. CONCLUSIONS

Considerable developments have taken place in the design of NIRS instrumentation since the technique was first described in 1977. These instruments potentially offer the hope of obtaining data on the absolute quantification of chromophore concentrations in tissue. Although the technologies involved will continue to improve, the major problem that remains is the accurate modelling of light transport in the complex heterogeneous structures that form real tissue, because quantification requires the fitting of measured data to some model prediction.

The authors thank all members of the Medical Optics Group in the Department of Medical Physics and Bioengineering, UCL, whose work has contributed to the results reported in this paper. This work was supported by grants from Action Research, Boehringer Mannheim, EPSRC, Hamamatsu Photonics KK and the Wellcome Trust.

REFERENCES

Aldrich, C. J., D'Antona, D., Wyatt, J. S., Spencer, J. A. D., Peebles, D. M. & Reynolds, E. O. R. 1994 Fetal cerebral oxygenation measured by near infrared spectroscopy shortly before birth and acid base status at birth. *Obstet. Gynec.* **84**, 861–866.

Arridge, S. R., Cope, M. & Delpy, D. T. 1992 Theoretical basis for the determination of optical pathlengths in tissue: temporal and frequency analysis. *Physics Med. Biol.* **37**, 1531–1560.

Arridge, S. R., Schweiger, M., Hiraoka, M. & Delpy, D. T. 1993 A finite element approach for modelling photon transport in tissue. *Med. Phys.* **20**, 299–309.

Bevilacqua, F., Marquet, P., Depeursinge, C. & de Haller, E. B. 1995 Determination of reduced scattering and absorption coefficients by a single charge coupled device array measurement. II. Measurement on biological tissues. *Opt. Engng* **34**, 2064–2069.

Brazy, J. E., Lewis, D. V., Mitnick, M. H. & Jobsis, F. F. 1985 Noninvasive monitoring of cerebral oxygenation in preterm infants: preliminary observations. *Pediatrics* **75**, 217–225.

Chance, B., Leigh, J. S., Miyake, H., Smith, D. S., Nioka, S., Greenfeld, R., Finander, M., Kaufmann, K., Levy, W., Young, M., Cohen, P., Yoshioka, H. & Boretsky, R. 1988*a* Comparison of time resolved and unresolved measurements of deoxhemoglobin in brain. *Proc. Natn. Acad. Sci. USA* **85**, 4971–4975.

Chance, B., Maris, M., Sorge, J. & Zhang, M. Z. 1990 A phase modulation system for dual wavelength difference spectroscopy of hemoglobin deoxygenation in tissues. *Proc. SPIE* **1204**, 481–491.

Chance, B., Nioka, S, Kent, J., McCully, K., Fountain, M., Greenfield, R. & Holtom, G. 1988*b* Time resolved spectroscopy of hemoglobin and myoglobin in resting and ischaemic muscle. *Analyt. Biochem.* **174**, 698–707.

Cheatle, T. R., Potter, L. A., Cope, M., Delpy, D. T., Coleridge-Smith, P. D. & Scurr, J. H. 1991 Near infrared spectroscopy in peripheral vascular disease. *Br. J. Surg.* **78**, 405–408.

Cheong, W. F, Prahl, S. A. & Welch, A. J. 1990 A review of the optical properties of biological tissues. *IEEE J. Quantum Electron.* **26**, 2166–2185.

Cooper, C. E., Elwell, C. E., Meek, J. H., Matcher, S. J., Wyatt, J. S., Cope, M. & Delpy, D. T. 1996 The noninvasive measurement of absolute cerebral deoxyhaemoglobin concentration and mean optical pathlength in the neonatal brain by second derivative near infrared spectroscopy. *Pediat. Res.* **39**, 32–38.

Cope, M. & Delpy, D. T. 1988 A system for long term measurement of cerebral blood and tissue oxygenation in newborn infants by near infrared transillumination. *Med. Biol. Engng Comp.* **26**, 289–294.

Cope, M., Delpy, D. T., Wray, S., Wyatt, J. S. & Reynolds, E. O. R. 1989 A CCD spectrometer to quantitate the concentration of chromophores in living tissue utilising the absorption peak of water at 975 nm. *Adv. Exp. Med. Biol.* **248**, 33–40.

Cope, M., Van der Zee, P., Essenpreis, M., Arridge, S. R. & Delpy, D. T. 1991 Data analysis methods for near infrared spectroscopy of tissue: problems in determining the relative cytochrome aa_3 concentration. *Proc. SPIE* **1431**, 251–262.

De Blasi, R. A. & Ferrari, M. 1995 Noninvasive measurement of forearm oxygen consumption by near infrared spectroscopy. *J. Appl. Physiol.* **78**, 1617–1618.

De Blasi, R. A., Ferrari, M., Natali, A., Conti, G, Mega, A. & Gasparetto, A. 1994 Noninvasive measurement of forearm blood flow and oxygen consumption by near infrared spectroscopy. *J. Appl. Physiol.* **76**, 1388–1393.

Delpy, D. T., Cope, M., Van der Zee, P., Arridge, S. R., Wray, S. & Wyatt, J. S. 1988 Estimation of optical pathlength through tissue from direct time of flight measurement. *Physics Med. Biol.* **33**, 1433–1442.

Duncan, A., Whitlock, T. L., Cope, M. & Delpy, D. T. 1993 A multiwavelength, wideband, intensity modulated optical spectrometer for near infrared spectroscopy and imaging. *Proc. SPIE* **1888**, 248–257.

Edwards, A. D., Wyatt, J. S., Richardson, C. E., Delpy, D. T., Cope, M. & Reynolds, E. O. R. 1988 Cotside measurement of cerebral blood flow in ill newborn infants by near infrared spectroscopy. *Lancet* ii, 770–771.

Elwell, C. E., Owen-Reece, H., Wyatt, J. S., Cope, M., Reynolds, E. O. R. & Delpy, D. T. 1996 Influence of respiration and changes in expiratory pressure on cerebral haemoglobin concentration measured by near infrared spectroscopy. *J. Cereb. Blood Flow Metab.* **16**, 353–357.

Essenpreis, M., Elwell, C. E., Cope, M., Van der Zee, P., Arridge, S. R. & Delpy, D. T. 1993 Spectral dependence of temporal point spread functions in human tissues. *Appl. Opt.* **32**, 418–425.

Fantini, S., Franceschini-Fantini, M. A., Maier, J. S., Walker, S. A., Barbieri, B. & Gratton, E. 1995 Frequency domain multichannel optical detector for noninvasive tissue spectroscopy and oximetry. *Opt. Engng* **34**, 32–42.

Farrell, T. J., Patterson, M. S. & Wilson, B. C. 1992 A diffusion theory model of spatially resolved steady state diffuse reflectance for the noninvasive determination of tissue optical properties *in vivo*. *Med. Phys.* **19**, 879–888.

Ferrari, M., De Marchis, C., Giannini, I., Di Nicola, A., Agostino, R., Nodari, S. & Bucci, G. 1986 Cerebral blood volume and hemoglobin oxygen saturation monitoring in neonatal brain by near IR spectroscopy. *Adv. Exp. Med. Biol.* **200**, 203–211.

Ferrari, M., Wilson, D. A., Hanley, D. F., Hartman, J. F., Traystman, R. J. & Rogers, M. C. 1989 Non invasive determination of haemoglobin saturation in dogs by derivative near infrared spectroscopy. *Am. J. Physiol.* **256**, H1493–H1499.

Firbank, M., Arridge, S. R., Schweiger, M. & Delpy, D. T. 1996 An investigation of light transport through scattering bodies with non scattering regions. *Physics Med. Biol.* **41**, 767–783.

Germon, T. J., Evans, P. D., Barnett, N. J., Wall, P. & Nelson, R. J. 1997 Multichannel NIRS analysis of intra and extracranial oxygenation changes. *Adv. Exp. Med. Biol.* (In the press.)

Germon, T. J., Kane, N. M., Manara, A. R. & Nelson, R. J. 1994 Near infrared spectroscopy in adults: effects of extracranial ischaemia and intracranial hypoxia on estimation of cerebral oxygenation. *Br. J. Anaesth.* **73**, 503–506.

Giannini, I., Ferrari, M., Carpi, A. & Fasella, P. 1982 Rat brain monitoring by near infrared spectroscopy: an assessment of possible clinical significance. *Physiol. Chem. Phys.* **14**, 295–305.

Groenhuis, R. A. J., Ferwerda, H. A. & Ten Bosch, J. J. 1993*a* Scattering and absorption of turbid materials determined from reflection measurements. I. Theory. *Appl. Opt.* **22**, 2456–2462.

Groenhuis, R. A. J., Ferwerda, H. A. & Ten Bosch, J. J. 1993*b* Scattering and absorption of turbid materials determined from reflection measurements. 2. Measuring method and calibration. *Appl. Opt.* **22**, 2463–2467.

Hasegawa, Y., Yamada, Y., Tamura, M. & Nomura, Y. 1991 Monte Carlo simulation of light transmission through living tissues. *Appl. Opt.* **30**, 4515–4520.

Haselgrove, J. C., Schotland, J. C. & Leigh, J. S. 1992 Long time behaviour of photon diffusion in an absorbing medium: application to time resolved spectroscopy. *Appl. Opt.* **31**, 2678–2683.

Hiraoka, M., Firbank, M., Essenpreis, M., Cope, M., Arridge, S. R., Van der Zee, P. & Delpy, D. T. 1993 A Monte Carlo investigation of optical pathlength in inhomogeneous tissue and its application to near infrared spectroscopy. *Physics Med. Biol.* **38**, 1859–1876.

Jöbsis, F. F. 1977 Noninvasive, infrared monitoring of cerebral and myocardial oxygen sufficiency and circulatory parameters. *Science* **198**, 1264–1267.

Kohl, M., Watson, R. & Cope, M. 1996 Determination of absorption coefficients in highly scattering media from changes in attenuation and phase. *Opt. Lett.* **21**, 1519–1521.

Lakowicz, J. R. & Berndt, K. 1990 Frequency domain measurement of photon migration in tissues. *Chem. Phys. Lett.* **166**, 246–252.

Lakowicz, J. R., Laczko, G. & Gryczynski, I. 1986 2 GHz frequency domain fluorometer. *Rev. Sci. Instrum.* **57**, 2499–2506.

Madsen, S., Anderson, E. R., Haskell, R. C. & Tromberg, B. J. 1994 Portable, high bandwidth frequency domain photon migration instrument for tissue spectroscopy. *Opt. Lett.* **19**, 1934 –1936.

Madsen, S. J., Wilson, B. C., Patterson, M. S., Park, Y. D., Jacques, S. J. & Hefetz, Y. 1992 Experimental tests of a simple diffusion model for estimation of scattering and absorption coefficients of turbid media from time resolved diffuse reflectance measurements. *Appl. Opt.* **31**, 3509–3517.

Marquet, P., Bevilacqua, F., Depeursinge, C. & de Haller, E. B. 1995 Determination of reduced scattering and absorption coefficients by a single charge coupled device array measurement. I. Comparison between experiments and simulations. *Opt. Engng* **34**, 2055–2063.

Matcher, S. J., Cope, M. & Delpy, D. T. 1994 Use of the water absorption spectrum to quantify tissue chromophore concentration changes in near infrared spectroscopy. *Physics Med. Biol.* **39**, 177–196.

Matcher, S. J., Cope, M. & Delpy, D. T. 1997 *In vivo* measurements of the wavelength dependence of tissue scattering coefficients between 760nm and 900nm measured using time resolved spectroscopy. *Appl. Opt.* **36**, 386–396.

Matcher, S. J., Elwell, C. E., Cooper, C. E., Cope, M. & Delpy, D. T. 1995*a* Performance comparisons of several published tissue near infrared spectroscopy algorithms. *Analyt. Biochem.* **227**, 54–68.

Matcher, S. J., Kirkpatrick, P., Nahid, K., Cope, M. & Delpy, D. T. 1995*b* Absolute quantification methods in tissue near infrared spectroscopy. *Proc. SPIE* **2389**, 486–495.

McCormick, P. W., Stewart, M., Goetting, M. G., Dujovny, M., Lewis, G. & Ausman, J. I. 1991 Noninvasive cerebral optical spectroscopy for monitoring cerebral oxygen delivery and haemodynamics. *Crit. Care Med.* **19**, 89–97.

Miwa, M., Ueda, Y. & Chance, B. 1995 Development of a time resolved spectroscopy system for quantitative noninvasive tissue measurement. *Proc. SPIE* **2389**, 142–149.

Oda, M., Yamashita, Y., Nishimura, G. & Tamura, M. 1996 A simple and novel algorithm for time resolved multiwavelength oximetry. *Physics Med. Biol.* **41**, 551–562.

Okada, E., Firbank, M. & Delpy, D. T. 1995 The effect of overlying tissue on the spatial sensitivity profile of near infrared spectroscopy. *Physics Med. Biol.* **40**, 2093–2108.

Okada, E., Firbank, M., Schweiger, M., Arridge, S. R, Cope, M. & Delpy, D. T. 1997 A theoretical and experimental investigation of near infrared propagation in a model of the adult head. *Appl. Opt.* **36**, 21–31.

Patterson, M. S., Chance, B. & Wilson, B. C. 1989 Time resolved reflectance and transmittances for the non invasive measurement of tissue optical properties. *Appl. Opt.* **28**, 2331–2336.

Patterson, M. S. & Pogue, B. W. 1994 Mathematical model for time resolved and frequency domain fluorescence spectroscopy in biological tissues. *Appl. Opt.* **10**, 1963–1974.

Peebles, D. M., Edwards, A. D., Wyatt, J. S., Bishop, A. P., Cope, M., Delpy, D. T. & Reynolds, E. O. R. 1992 Changes in human fetal cerebral haemoglobin concentration and oxygenation during labour measured by near infrared spectroscopy. *Am. J. Obstet. Gynec.* **166**, 1369–1373.

Pollard, V., Prough, D. S., DeMelo, A. E., Deyo, D. J., Uchida, T. & Stoddart, H. F. 1996 Validation in volunteers of a near infrared spectroscope for monitoring brain oxygenation in vivo. *Anesth. Analg.* **82**, 269–277.

Proc. SPIE 1991 **1431**.

Proc. SPIE 1993 **1888**.

Proc. SPIE 1995 **2389**.

Sevick, E. M., Frisoli, J. K., Burch, C. L. & Lakowicz, J. R. 1994 Localisation of absorbers in scattering media by use of frequency domain measurements of time dependent photon migration. *Appl. Opt.* **33**, 3562–3570.

Skov, L., Pryds, O., Greisen, G. & Lou, H. 1993 Estimation of cerebral venous saturation in newborn infants by near infrared spectroscopy. *Pediat. Res.* **33**, 52–55.

Van der Zee, P., Cope, M., Arridge, S. R., Essenpreis, M., Potter, L. A., Edwards, A. D.

Wahr, J. A., Tremper, K. T., Samra, S. & Delpy, D. T. 1996 Near infrared spectroscopy: theory and applications. *J. Cardiothoracic Vasc. Anesth.* **10**, 406–418.

Wickramsinghe, Y. A. B. D., Crowe, J. A. & Rolfe, P. 1986 Laser source and detector with signal processor for a near infrared medical application. In *Progress reports on electronics in medicine & biology* (ed. K. Copeland), pp. 209–215. London: IERE Press.

Wilson, B. C. & Adam, G. 1983 A Monte Carlo model for the absorption and flux distributions of light in tissue. *Med. Phys.* **10**, 824–830.

Wray, S., Cope, M., Delpy, D. T., Wyatt, J. S. & Reynolds, E. O. R. 1988 Characterisation of the near infrared absorption spectra of cytochrome aa_3 and haemoglobin for

the non invasive monitoring of cerebral oxygenation. *Biochem. Biophys. Acta* **933**, 184–192.

Wyatt, J. S., Cope, M., Delpy, D. T., Richardson, C. E., Edwards, A. D., Wray, S. C. & Reynolds, E. O. R. 1990 Quantitation of cerebral blood volume in newborn infants by near infrared spectroscopy. *J. Appl. Physiol.* **68**, 1086–1091.

Wyatt, J. S., Cope, M., Delpy, D. T., Wray, S. & Reynolds, E. O. R. 1986 Quantification of cerebral oxygenation and haemodynamics in sick newborn infants by near infrared spectrophotometry. *Lancet* **2**, 1063–1066.

Wyatt, J. S., McCormick, D. C., Roth, S. C., Reynolds, E. O. R. & Delpy, D. T. 1992 Experimentally measured optical pathlengths for the adult head, calf and forearm and the head of the newborn infant as a function of interoptode spacing. *Adv. Exp. Med. Biol.* **316**, 143–153.

Yamada, Y., Hasegawa, Y. & Maki, H. 1993*a* Simulation of time resolved optical computer tomography imaging. *Opt. Engng* **32**, 634–641.

Yamada, Y., Hasegawa, Y. & Yamashita, Y. 1993*b* Simulation of fan beam type optical CT imaging of strongly scattering and weakly absorbing media. *Appl. Opt.* **32**, 4808–4814.

Yoxall, C. W., Weindling, A. M., Dawani, N. H. & Peart, I. 1995 Measurement of cerebral venous oxyhaemoglobin saturation in children by near infrared spectroscopy and partial jugular venous occlusion. *Pediat. Res.* **38**, 319–323.

PHILOSOPHICAL TRANSACTIONS OF THE ROYAL SOCIETY B BIOLOGICAL SCIENCES